

## Supplemental Material

### Regulatory T cells contribute to sexual dimorphism in neonatal hypoxic-ischemic brain injury

Lucia Beckmann (MD)<sup>\*1,2</sup>, Stefanie Obst (MSc)<sup>\*1,2</sup>, Nicole Labusek (MSc)<sup>\*1,2</sup>, Hanna Abberger (PhD)<sup>3</sup>, Christian Köster<sup>1,2</sup>, Ludger Klein-Hitpass (PhD)<sup>4</sup>, Sven Schumann (MD)<sup>5</sup>, Christoph Kleinschnitz (MD)<sup>2,6</sup>, Dirk M. Hermann (MD)<sup>2,6</sup>, Ursula Felderhoff-Müser (MD)<sup>1,2</sup>, Ivo Bendix (PhD)<sup>1,2</sup>, Wiebke Hansen (PhD)<sup>3</sup>, Josephine Herz (PhD)<sup>1,2#</sup>

<sup>1</sup> Department of Pediatrics I, Neonatology & Experimental Perinatal Neurosciences, University Hospital Essen, University Duisburg-Essen, Essen, Germany

<sup>2</sup>Center for Translational Neuro- and Behavioral Sciences (C-TNBS)

<sup>3</sup> Institute of Medical Microbiology, Molecular Infection Immunology, University Hospital Essen, University Duisburg-Essen, Essen, Germany

<sup>4</sup> Institute of Cell Biology, Genomic and Transcriptomic Facility (GTF), University Hospital Essen, University Duisburg-Essen, Essen, Germany

<sup>5</sup> Institute for Microscopic Anatomy and Neurobiology, University Medical Center, Johannes Gutenberg-University, Mainz, Germany

<sup>6</sup> Department of Neurology, University Hospital Essen, University Duisburg-Essen, Essen, Germany

#### Content

<u>Supplemental Material and Methods:</u>	1
<u>Supplemental Figures:</u>	9
<u>Supplemental Tables:</u>	6 (2 Tables (IV and VI) provided as excel sheets)

**#Corresponding author:** Josephine Herz  
Department of Pediatrics I  
Neonatology & Experimental Perinatal Neurosciences  
University Hospital Essen, University Duisburg-Essen  
Hufelandstr. 55  
45147 Essen  
Email: [josephine.herz@uk-essen.de](mailto:josephine.herz@uk-essen.de)  
Phone: +49 201 723 85187

## **Supplemental Methods**

### **Animal allocation**

For all analyses, animals per litter and experiment were randomly assigned to experimental groups prior to intervention. To control the potential influence of weight and sex a stratified randomization was performed followed by simple randomization within each block to assign pups to individual groups (PBS, DTX). Individuals involved in data analysis knew the animals' designation but were blinded to group assignment. Details on animals' genotype, sex, group assignment and mortality are provided in Supplemental Table I.

### **Genotyping of DEREg mice**

DNA was isolated from tail biopsies 2 days prior to intervention by the DNeasy Blood and Tissue kit (Qiagen, Germany) according to the manufacturers' protocol ("Purification of Total DNA from Animal Tissue"). The quality of isolated DNA was checked by spectrophotometry followed by PCR with the following primers: Fwd 1 GCGAGGGCGATGCCACCTACGGCA, Rev 1 GGGTGTCTGCTGGTAGTGGTCCG, Fwd 2 CCCAGGTTACCATGGAGAGA, Rev2 GAACTTCAGGGTCAGCTTGC. PCR products were separated by gel electrophoresis and transgenic mice were identified by a single band at 500 bp.

### **Histopathological examination of peripheral organs 5 weeks after Treg depletion**

Animals were anesthetized by i.p. injection of an overdose chloral hydrate, followed by transcardial perfusion with PBS. Spleens and lymph nodes were isolated and kept on ice until further processing. Following PBS perfusion, animals were perfused with 4% PFA and skin, lung, liver and pancreas tissues were dissected followed by fixation in 4% PFA at 4°C overnight. Organs were embedded in paraffin and cut into 10 µm tissue sections followed by haematoxylin/eosin (HE) staining. HE stained tissue sections of peripheral organs were analysed by an anatomist for signs of autoimmune reactions, e.g. immune cell infiltrates. Spleen and lymph node samples were homogenized through a 70 µm cell strainer (BD Biosciences, Germany) by continuous rinsing with 15 mL of cold HEPES-buffered RPMI1640 (Gibco, Thermo Scientific, USA). Living cell numbers were determined with a hemacytometer after trypan blue staining.

### **Flow cytometry and suppression assays**

Ipsilateral brain hemispheres and spleens were dissected and homogenized through a 70 µm cell strainer (BD Biosciences) by continuous rinsing with 15 mL of cold HEPES-buffered RPMI1640 (Gibco, Thermo Scientific). Brain samples were centrifuged at 400xg for 10 minutes at 18°C. The supernatants were discarded and the pellets were resuspended in 15 mL of 37% Percoll (Sigma Aldrich, Germany) in 0.01 N HCl/PBS and centrifuged at 2800xg for 20 minutes. Myelin was removed and the remaining cell pellet was washed twice in PBS. Erythrocytes in spleen and blood samples were lysed by incubation with lysis buffer (155 mM NH<sub>4</sub>Cl, 10 mM KHCO<sub>3</sub>, 3 mM EDTA) for 5 minutes followed by two washing steps with PBS.

Isolated cells were incubated with five antibody cocktails (Supplementary Table II) for 20 minutes at 4°C. For analyses of Treg numbers and frequencies in C57BL/6 mice (Panel 1), surface staining was followed by intracellular staining with the Foxp3 intracellular staining kit (eBioscience, Germany) according to the manufacturers' protocol. Viable leukocytes were identified by gating for CD45<sup>high</sup> cells and FVD (fixable viability dye, eBioscience) negative cells. Within this subset, Tregs were identified as CD3<sup>+</sup>CD8<sup>-</sup>CD4<sup>+</sup>Foxp3<sup>+</sup> cells. Total cell counts were determined using BD TrueCount beads (BD Biosciences). Depletion efficiency and recovery of Tregs were analysed with staining Panel 2. Chemokine and integrin expression was assessed in CD45<sup>+</sup>CD3<sup>+</sup>CD4<sup>+</sup>Foxp3eGFP cells with Panel 3 and 4. Gates for chemokine and integrin expression analyses were set according to fluorescent minus one controls for each organ.

The suppressive activity of Tregs on effector T cell proliferation was analysed in *ex vivo* sorted Tregs. Briefly, isolated spleen cells transgenic DEREg mice were incubated with anti-CD4 and anti-CD8 (Supplemental Table II, Panel 5) for 10 minutes at 4°C followed by cell sorting of CD4<sup>+</sup>CD8<sup>-</sup>Foxp3eGFP cells with a FACS Aria II (BD Biosciences). Effector T cells were isolated from the spleen of a CD45.1 mouse by magnetic activated cell sorting using the CD4

T cell isolation kit (Miltenyi Biotec, Germany) according to the manufacturers' protocol. Effector T cells were stained with 8 ng/μl eFluor 670 for 10 min at 37°C followed by incubation with fetal calf serum (FCS, PAA Laboratories, Austria) for 5 min on ice. Sorted Tregs ( $1.5 \times 10^4$ ) were co-incubated with irradiated antigen presenting cells ( $6 \times 10^4$ ), derived from a spleen of a C57BL/6 mouse, labelled effector T cells ( $1.5 \times 10^4$ ) and 1 μg/μl anti-CD3 (BD Bioscience) in 200 μl IMDMc medium (Gibco Thermo Scientific) supplemented with 25 mM HEPES (Gibco Thermo Scientific), 10% FCS, 1% Penicillin/Streptavidin (Sigma Aldrich, Germany) and 25 μM beta-Mercaptoethanol (Carl Roth, Germany) for 4 days at 37°C, 5% CO<sub>2</sub>. Effector T cell proliferation was analysed by flow cytometry after staining the cell suspension with anti-CD45.1 and anti-CD4 (Supplemental Table II, Panel 5). Gates to determine the percentage of proliferated cells were set according to unstimulated controls. The percentage of inhibition was calculated according to stimulated controls without Tregs.

To determine the suppressive capacity of Tregs on myeloid cell activation, in addition to GFP<sup>+</sup> Tregs, CD11b<sup>+</sup> myeloid (both Ly6G<sup>+</sup> and Ly6G<sup>-</sup>) cells were sorted (Panel 6). 50.000 myeloid cells were co-incubated with 10.000 Tregs and stimulated with 12.9 mM PMA (phorbol 12-myristate 13-acetate, Biomol, Hamburg, Germany) in DMEM, 1% penicillin/streptomycin (Gibco, Thermo Fisher Scientific, Waltham, U.S.), 10% FCS (Biochrom, Merck, Darmstadt, Germany) for 30 min at 37°C. Unstimulated control cells were incubated with medium and without Tregs. Stimulated control cells were incubated with PMA and without Tregs. After stimulation, cells were stained with 2.5 μg/ml Dihydrorhodamine 123 (Sigma-Aldrich/Merck, Darmstadt, Germany) for 15 min at 37°C followed by one washing step prior to measurement. To separate responses of neutrophils (Ly6G<sup>+</sup>) and other myeloid cells (mainly macrophages and monocytes), gates were set to CD11b<sup>+</sup>Ly6G<sup>+</sup> and CD11b<sup>+</sup>Ly6G<sup>-</sup> cells, after exclusion of CD4 PE-Cy7 cells. Mean fluorescence intensities of unstimulated controls were subtracted from values of stimulated controls and the percentage of inhibition in samples with Tregs was calculated according to stimulated controls without Tregs.

All flow cytometry measurements and analyses were performed with the LSRII and BD Diva Software (both BD Biosciences), respectively. Details about antibodies and dyes used in the present study are provided in Supplemental Table II.

### **Immunohistochemistry**

Brain tissue injury was assessed and scored on cresyl violet stained 20 μm cryostat sections as we have previously described<sup>1-3</sup>. Briefly, nine regions were scored: the anterior, middle, and posterior cortex, CA1, CA2, CA3, and dentate gyrus of the hippocampus, thalamus and the striatum. Each region was given a rating from 0 to 3 (0 - no detectable cell loss, 1 - small focal areas of neuronal cell loss, 2 - columnar damage in the cortex or moderate to severe cell loss in the other regions, 3 - cystic infarction and gliosis). The sum score for different regions was calculated.

Detailed information on primary antibodies used for immunohistochemistry, is provided in supplemental Table III. For evaluation of Treg infiltration, neuronal loss, glial activation, vascular integrity and leukocyte infiltration, tissue sections were thawed at 37°C for 15 min followed by fixation with either 1:1 Aceton/Methanol for 3 min (anti-Laminin, anti-CD31, anti-eGFP, anti-CD45, anti-CD41, anti-von Willebrand Factor (vWF)) or 4%PFA for 5 min (anti-NeuN, anti-Olig2). For simultaneous visualization of microglia and astrocytes in native tissue sections, sections had to be fixed for 4h in 4% PFA followed by antigen retrieval in citrate buffer (10 mM sodium citrate, 0.05% Tween 20, ph 6) for 10 min at 100°C. Unspecific antibody binding was blocked by incubation either with 5% normal goat serum (anti-eGFP, anti-CD45, anti-Laminin, anti-CD31, anti-Iba-1, anti-GFAP) or 1% bovine serum albumine, 0.3% fish gelatin (anti-NeuN, anti-Olig2, anti-CD41, anti-vWF, anti-Laminin) both in 0.2% Tween 20 in PBS for 1 hour at room temperature. Primary antibodies were incubated in either 1% NGS (anti-eGFP, anti-CD45, anti-Laminin, anti-CD31, anti-Iba-1, anti-GFAP) or 1% bovine serum albumine, 0.3% fish gelatin (anti-NeuN, anti-Olig2, anti-CD41, anti-vWF, anti-Laminin) both in 0.2% Tween 20 in PBS overnight. Antibody binding was visualized by incubation with appropriate Alexa Fluor 488, Alexa Fluor 555 and Alexa Fluor 647 conjugated secondary antibodies (anti-rat/rabbit/sheep, all 1:500, all Thermo Scientific) in PBS for 2 hours at room

temperature. Nuclei were counterstained with 4',6-Diamidin-2-phenylindol (DAPI, 100 ng/ml; Molecular Probes, USA). Cellular degeneration was assessed by terminal transferase dUTP nick end labeling (TUNEL) according to the manufacturer's protocol (In situ Cell Death Detection Kit, Roche, Switzerland).

### **Quantification of Treg infiltration, cellular degeneration, neuronal loss, glial activation, vascular integrity, leukocyte infiltration, platelet counts and vWF immunoreactivity**

Conventional fluorescence microscopy (40x objective; Axioplan connected to a CCD camera (Axiocam ICc1), Zeiss, Germany) and confocal imaging (10x and 20x objective, A1plus, Eclipse Ti, with NIS Elements AR software, Nikon, Germany) were applied.

Treg infiltration was quantified in eGFP/CD45 co-staining. Tregs were counted in the total ipsilateral hemisphere at the level of the hippocampus (-1.9 to -2.0 mm from bregma) and striatum (+0.2 to +0.3 mm from bregma). In each level 16 tissue sections per animal were analysed and mean values calculated. In each group 5 animals were randomly selected prior to cell counting to visualize the location of Tregs (Fig. 1C). The sum of Tregs of 16 sections per level of these 5 animals are depicted in the brain graphics of Fig. 1C of the main manuscript. These 5 animals were also used to determine distances of Tregs from the vasculature in 8 sections / animal stained for eGFP and CD31. Analysis was performed by confocal microscopy in 10  $\mu\text{m}$  z-stacks (z-distance 2  $\mu\text{m}$ ). Distances to the next adjacent vessel were measured in maximal intensity projections with the NIS Elements AR software. All Tregs overlapping with a CD31 signal were counted as "intravascular" Tregs. A total of 96 female and 34 male Tregs was analysed.

Neuronal and oligodendrocyte density, vascular integrity and leukocyte infiltration were quantified according to our previous reports<sup>2,3</sup>. Briefly, images of 3 defined non-overlapping regions of interest (ROI, each 45,900  $\mu\text{m}^2$ ) in each brain region were acquired. Oligodendrocytes were counted manually on acquired images. Since single cell counting could not be applied in densely packed regions of neurons or strong leukocyte infiltration (e.g. hippocampus), images were converted into binary images followed by measurement of NeuN and CD45 positive areas using Image J (NIH, USA). To quantify vascular injury, Laminin<sup>+</sup> areas were quantified as a measure of vascular integrity, since HI causes dilation and loosening of basal membranes as we have previously described<sup>3</sup>. Neuronal and oligodendrocyte densities and basal membrane disruption were determined in ipsilateral hemispheres of HI-injured and sham-operated animals. Since sham animals did not reveal significant group differences (Supplemental Fig. IV), median, 25<sup>th</sup> and 75<sup>th</sup> percentile values of pooled sham data are presented in the figures of the main manuscript as dashed lines and grey shadows. Peripheral leukocytes were hardly detectable in brains of sham-operated animals; and if so, all of them were found in the vessels (Supplemental Fig. VIII B). However, in HI-injured animals we observed a significant perivascular and intra-parenchymal accumulation of peripheral leukocytes (Fig. 3 D,E). To determine whether Tregs modulate extravasation behaviour of peripheral leukocytes, we evaluated leukocyte localization in Treg-depleted animals in CD45/Laminin stained tissue sections using confocal imaging (20x objective, 2  $\mu\text{m}$  focal plane distance in a total z-stack of 10  $\mu\text{m}$ ) in 3 non-overlapping randomly selected ROIs (each 90,000  $\mu\text{m}^2$ ) in peri-infarct areas of the hippocampus, where single cell detection was possible (Fig. 3 E). Cells with distances smaller than 10  $\mu\text{m}$  were qualified as intra/perivascular cells and the percentage of these cells from total leukocytes was calculated for each animal (Fig. 3E left). Distances of leukocytes located larger than 10  $\mu\text{m}$  apart from the next adjacent vessel were quantified (Fig. 3E right).

Confocal imaging with the perfect focus system module (A1plus, Eclipse Ti, with NIS Elements AR software, Nikon, Germany) was also used to generate large scale images (stitching) of the total hippocampus to determine apoptosis, microglia and astrocyte activation in TUNEL, Iba-1 and GFAP-stained tissue sections, respectively. Using the 10x objective with z-stacks of 12  $\mu\text{m}$  thickness (3  $\mu\text{m}$  focal plane distance) were acquired in 7 x 6 overlapping regions (15% overlap). Images were converted into maximal intensity projections for unbiased automated software-based quantification of TUNEL<sup>+</sup> cells using the NIS Elements AR software. Single object counting was not possible for Iba-1 and GFAP staining due to high cellular densities in

severely injured animals. Therefore, positively stained areas were quantified as a measure of cellular activation. Quantification of micro- and astroglia was performed in ipsilateral hemispheres of HI-injured and sham-operated animals. Since sham animals did not reveal significant group differences for these analyses (Supplemental Fig. VII), median, 25<sup>th</sup> and 75<sup>th</sup> percentile values of pooled sham data are presented in the figures of the main manuscript as dashed lines and grey shadows.

To analyse platelet CD41 and von Willebrand Factor (vWF) immunoreactivity as markers of thromboinflammation, 3 non-overlapping ROIs (each: 369.900  $\mu\text{m}$ ) in the hippocampus were acquired and vessel-associated platelets were counted manually. vWF immunoreactivity was analysed by measurement of positively stained areas.

### **Behavioral assessment**

Short (3 days) and long-term (5 weeks) behavioral outcome was assessed according to previous studies, including our own<sup>2, 4</sup>. Briefly, short-term motor coordination deficits were determined in the front-limb suspension test as previously described<sup>4</sup>. For evaluation of long-term neurodevelopment, animals were transferred to an inverted light/dark cycle after weaning. All following experimental procedures were carried out in the dark phase in a dimly lit (red light) and a low noise environment (behavioral unit). Long-term neurodevelopmental outcome was evaluated in the *Elevated Plus Maze (EPM)* and *Novel Object Recognition (NOR)* task according to our previous report<sup>2</sup>. Exploration and impulsive behavior were assessed in the *EPM*, where mice were placed on the central platform and behavior was recorded for 5 min. The time spent in the open arms and the time of head-dipping in open and center regions was measured. The *NOR* task is a non-spatial, non-aversive memory test, relying on the observation, that animals preferentially explore novel objects over those that are familiar. In the initial familiarization/training trial, animals were placed in the open field arena, exposed to 2 identical objects in two facing corners to determine general exploratory activity. The animals were returned to their cages for an inter-trial interval of 30 min. In the following retention/test trial, animals were exposed to one familiar object and one novel object replacing the second familiar object in the arena. Novel object activity was recorded for 5 min. All data were recorded using an automatic tracking system (Noldus, Germany) and exported for statistical analysis.

### **Western Blot**

Brain tissues were homogenized in ice-cold lysis buffer (RIPA, Sigma-Aldrich) containing protease and phosphatase inhibitors (cOmplete, Roche) and 100 mM PMSF (Sigma-Aldrich). The supernatant was collected and processed as previously described<sup>1</sup>. Protein lysates were separated on 12.5% sodiumdodecylsulphate (SDS) polyacrylamide gels and transferred to nitrocellulose membranes (0.2  $\mu\text{m}$ , Amersham, USA) at 4°C overnight. Equal loading of 20  $\mu\text{g}$ /lane and protein transfer was confirmed by staining of membranes with Ponceau S solution (Sigma-Aldrich). Nonspecific binding was blocked by incubation in 5% non-fat milk powder, 0.1% Tween in TBS (TBST). Membranes were incubated with the following primary antibodies: goat anti-vascular cell adhesion molecule-1 (VCAM-1, 1:10,000, R&D Systems, USA), rabbit anti-Iba-1 1:1,000, Wako, Japan), biotinylated goat anti-mouse ICAM-1 (1:10,000, R&D Systems) and rabbit anti-glutaraldehyde-3-phosphate dehydrogenase (GAPDH, 1:1,000, Santa Cruz, CA, USA) as reference protein. Antibody binding was detected by incubation with appropriate peroxidase-conjugated secondary antibodies (all 1:2,000 except of anti-goat HRP (1:10,000), all Dako, Denmark) in blocking solution at room temperature for 1 h. For detection of ICAM-1, the Vectastain ABC-HRP Kit (Vector Laboratories, USA) was used according to the manufacturers' instructions. Antibody binding was revealed by chemiluminescence using the enhanced chemiluminescence prime western blotting detection reagent (Amersham, GE Healthcare Life Science, USA). For visualization and densitometric analysis, the ChemiDocXRS+ imaging system and ImageLab software (Bio-Rad, Germany) were used. Pixel intensities were related to GAPDH and normalized to ratios of PBS-treated female mice.

### **Microarray analysis**

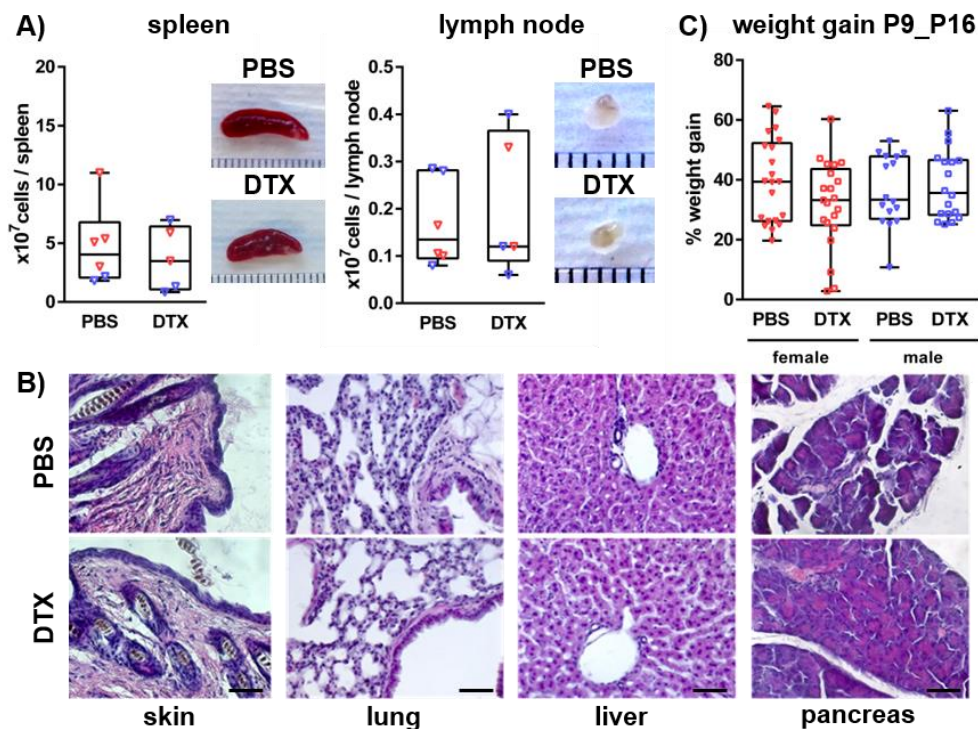
Target preparation was performed according to the Affymetrix WT Pico Expression Protocol for analyses on the Affymetrix Clariom S mouse array (eBioscience). Hybridization, washing and staining of the arrays was done according to the Affymetrix recommendations on the GC

Scanner 3000 with G7 update. Male samples were compared to respective baseline samples (i.e. females) by using the RMA signal summarization method and ANOVA test implemented in PartekGS v7.18. Tregs of 2 mice were pooled per sample and 3 samples per group were included in analysis. This exploratory analysis aimed to get first important insights into global pathways differing between female and male Tregs. Therefore, the present study focused on gene set enrichment analysis (GSEA), specifically on the hallmark gene set collection of the Molecular Signature Database (MSigDB)<sup>5</sup>. The entire data set with signal intensities is provided in a separate excel sheet (Supplemental Table VI).

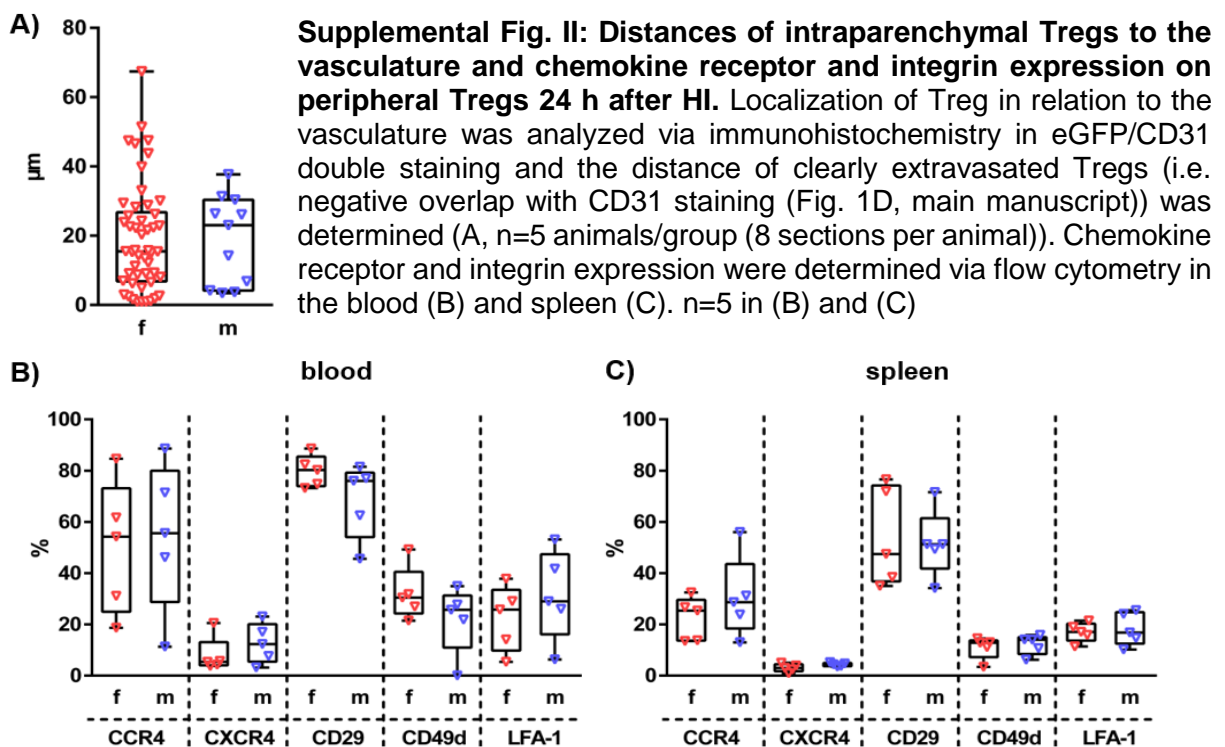
### **Estradiol measurement**

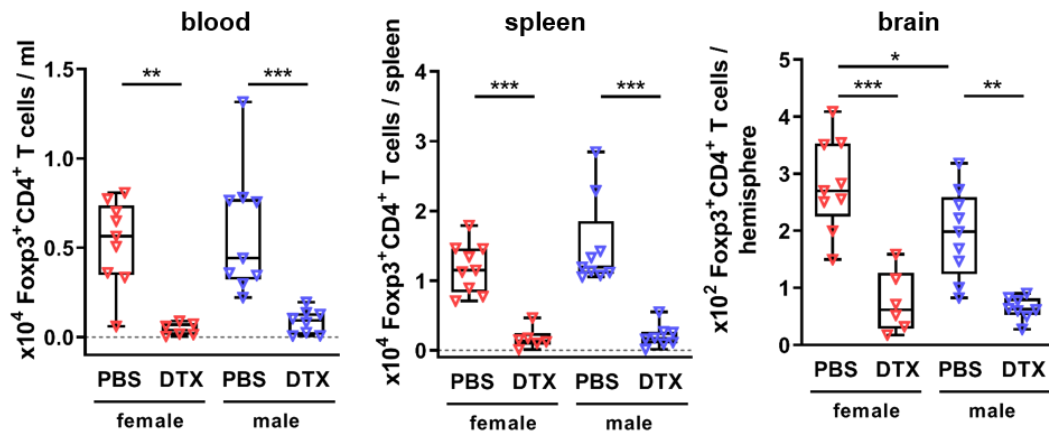
Blood was collected from the right atrium prior to perfusion and incubated for at least 30 min at room temperature prior to centrifugation for 15 min at 1000xg. Supernatants were frozen at -80°C until further analyses. Estradiol concentrations were quantified with the Parameter™ Estradiol Assay Kit (R&D Systems) according to the manufacturers' protocol.

## Supplemental Figures

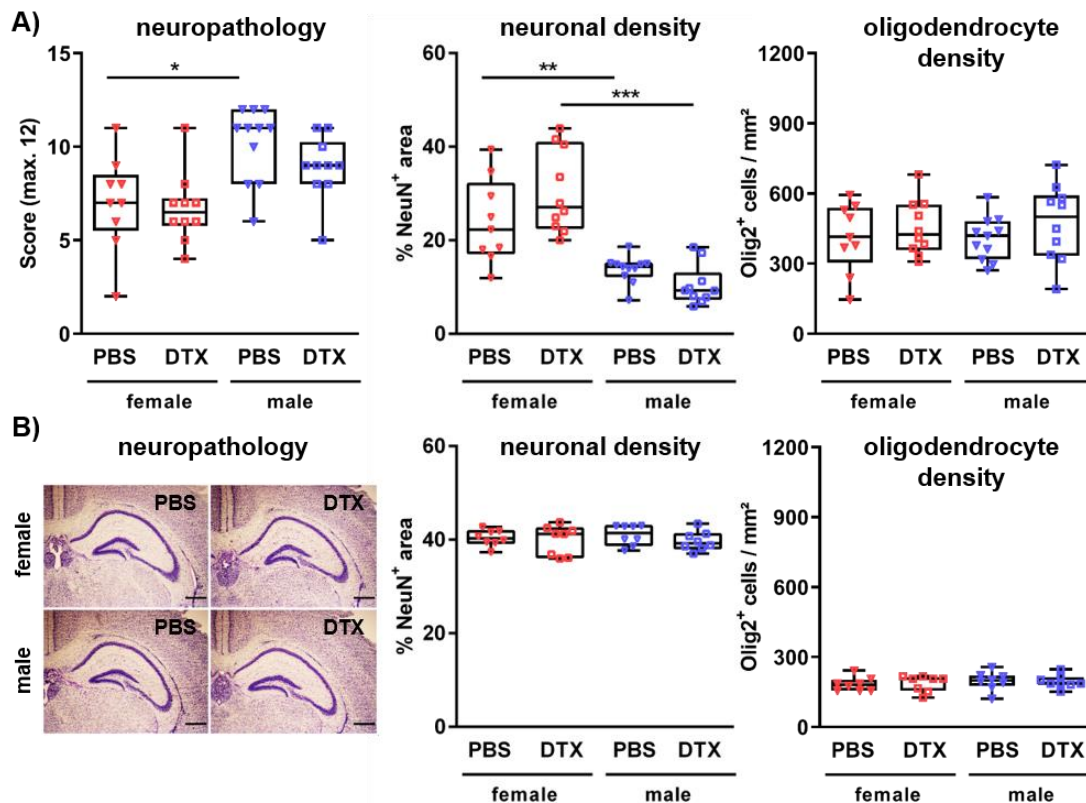


**Supplemental Figure I: Short neonatal Treg depletion neither leads to long-term autoimmune reactions nor modulates developmental weight gain.** DEREK mice were injected with 30 ng/g bodyweight DTX or PBS at postnatal day 8 (P8) and P10. Spleens and lymph nodes were analyzed for hyperplasia (A) and peripheral organs were evaluated for autoimmune reactions in HE-stained tissue sections (B, scale bar: 50  $\mu$ m), revealing no differences between both treatments for all animals analyzed. Images in (B) are representative for all mice included in analysis (n=5-6/group). Developmental weight gain in HI-injured animals was also not modulated in this experimental setting (C, n=37-39). Red and blue dots in (A) indicate female and male mice, respectively.

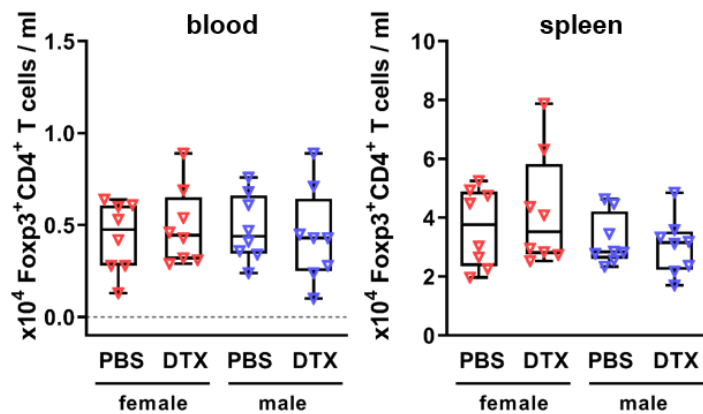




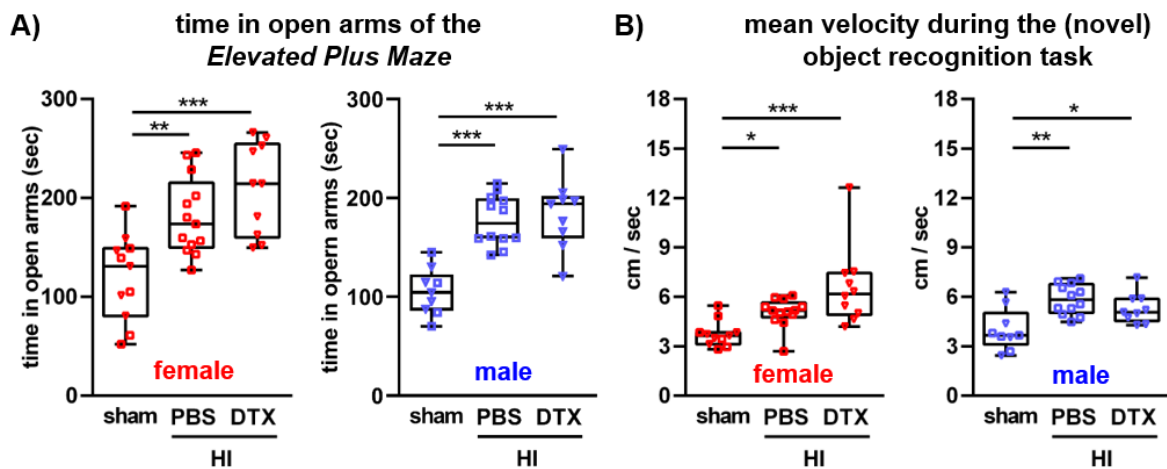
**Supplemental Fig. III: Treg depletion efficiency 48 hours after a single DTX injection.** Treg depletion efficiency was analyzed 48 h after a single injection of 30 ng/g body weight DTX or PBS into P8 DEREG mice, i.e. 1 day prior to HI. Tregs were quantified via flow cytometry applying CD4/Foxp3 staining (Panel 2, Supplemental Table II). Analyses in blood, spleen and brains 1 day after HI revealed a significant reduction of peripheral and cerebral Tregs, which did not differ between sexes. Confirming results obtained in C57Bl/6 animals (Fig. 1A), males reveal a significantly reduced amount of infiltrated Tregs in HI-injured hemispheres. n=6-9/group.



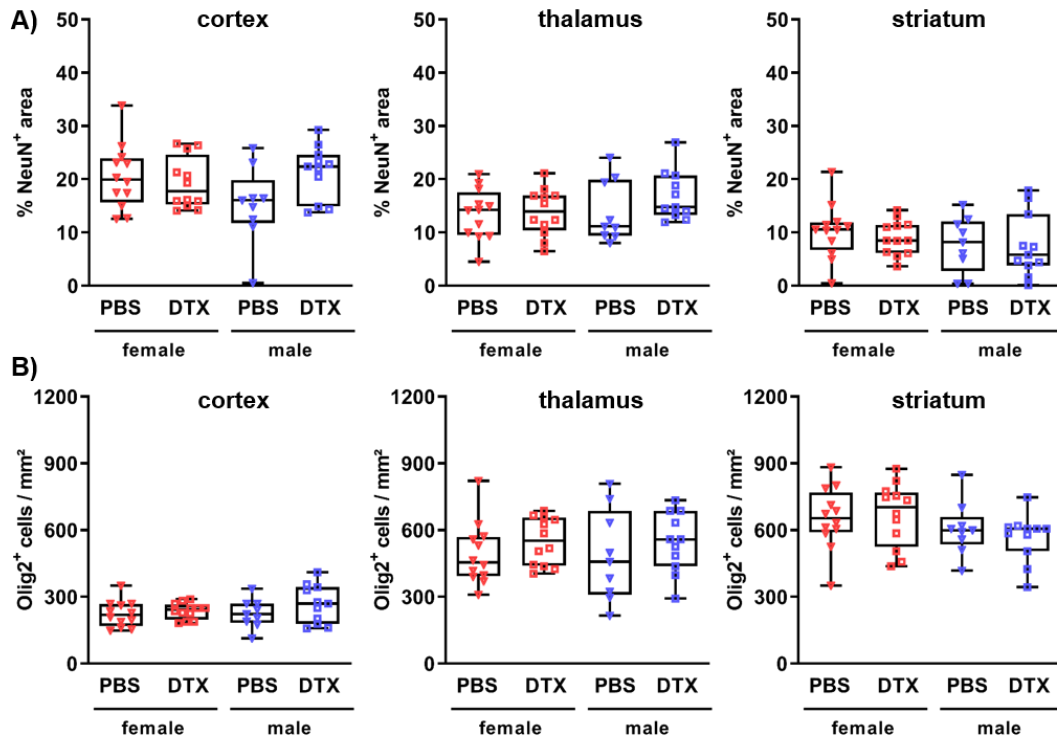
**Supplemental Fig. IV: DTX injection neither modulates HI-induced brain injury in wildtype littermates nor induces neuropathological changes in uninjured transgenic DEREG mice.** P9 wildtype littermates (A) and transgenic DEREG mice (B) were exposed to HI (A) and sham operation (B), respectively. 30 ng/g bodyweight DTX were i.p. injected at P8 and P10. At P16 histological examination was performed in cresyl violet stained tissue sections, neuronal and oligodendrocyte densities were analysed via immunohistochemistry for NeuN and Olig2. Except of an increased HI-induced brain injury in male animals, confirming results obtained in transgenic DEREG mice (Fig. 2A,B), no differences were caused by DTX injection. Scale bar (B): 0.5 mm, n=9-11/group in (A), n=8/group in (B)



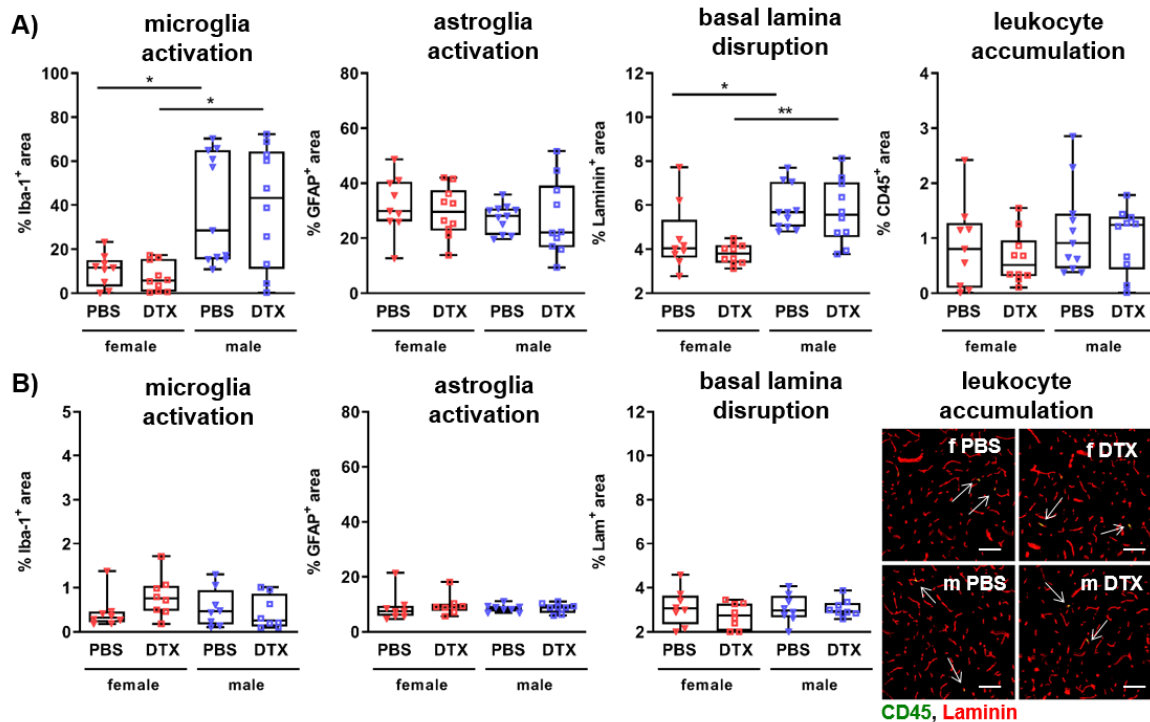
**Supplemental Fig. V: Treg recovery 6 days after DTX injection is similar in females and males.** Treg numbers were quantified via flow cytometry in blood and spleen 6 days after the second DTX injection in P10 DERE mice. Both female and males reveal a similar recovery of peripheral T cells, resulting in comparable numbers to PBS-treated control animals. n=8/group



**Supplemental Fig. VI: Neonatal HI reduces anxiety / enhances impulsivity and escape behaviour in young female and male adult mice, which is not modulated by neonatal Treg depletion.** P9 transgenic DERE mice were exposed to HI or sham operation. Treg depletion was induced by i.p. injections of 30 ng/g diphtheria toxin at P8 and P10. Animals were transferred to an inverted light/dark cycle after weaning. Five weeks after injury neurobehavioral testing was performed in the *Elevated Plus Maze*, measuring the time, the animals spent in the open arms (A) and in the *Novel Object Recognition* (B). Mean velocities were measured in the training (two identical objects) and the testing trial (one novel, one familiar object), the mean of both trials is depicted in (B). Symbols in sham-animals: rectangle=PBS, triangle=DTX. n=9-13/group

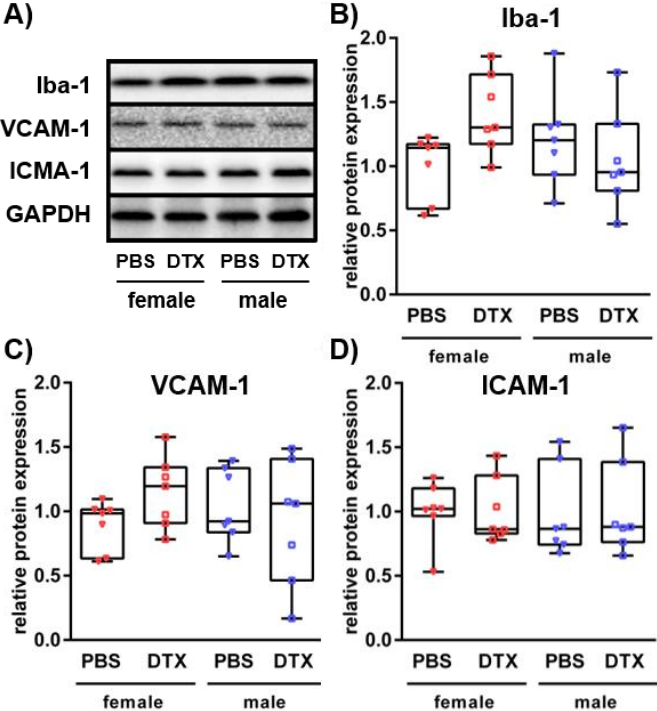


**Supplemental Fig. VII: Treg depletion does not influence neuronal and oligodendrocyte density in the cortex, thalamus and striatum.** P9 DEREg mice were exposed to HI. Treg depletion was induced by i.p. injections of 30 ng/g bodyweight DTX at P8 and P10. At P16 neuronal (A) and oligodendrocyte (B) densities were analysed via immunohistochemistry for NeuN and Olig2. n=9-12/group.



**Supplemental Fig. VIII: DTX injection neither modulates HI-induced glial activation, leukocyte infiltration and basal lamina disruption in wildtype littermates nor induces inflammatory responses and vascular injury in uninjured transgenic DEREg mice.** P9 wildtype littermates (A) and transgenic DEREg mice (B) were exposed to HI (A) and sham operation (B), respectively. 30 ng/g bodyweight DTX were i.p. injected at P8 and P10. At P16

microglia and astroglia activation, basal lamina disruption and leukocyte accumulation were determined via immunohistochemistry for Iba-1, GFAP, Laminin and CD45, respectively. Except of an increased HI-induced microglia activation and basal lamina disruption in male animals, confirming results obtained in transgenic DEREg mice (Fig. 3A,C), no significant differences were caused by DTX injection. A slight, non-significant increase in microglia-activation was observed in DTX-treated sham-operated females and males independent of DTX (B), which was however negligible small compared to responses in HI-injured animals (A, Fig. 3A). In sham-operated animals CD45 leukocytes were hardly detectable and if so, they were mainly found in the vessels (arrows in B). Scale bar (B): 100  $\mu$ m. n=9-11/group in (A), n=8/group in (B).



**Supplemental Fig. IX: Early impact of Treg depletion on microglia and endothelial activation.** P9 DEREg mice were exposed to HI. Tregs were depleted by i.p. injection of 30 ng/g bodyweight DTX at P8 and P10. At P11 microglia and endothelial activation were assessed by quantification of Iba-1 (A,B), VCAM-1 (A,C) and ICAM-1 expression (A,D) *via* western blot. Data were normalized to the reference protein GAPDH (A) and to PBS-treated female mice. n=7/group

## Supplemental Tables

**Supplemental Table I: Group allocation and mortality**

Readout / experiments / groups	female	male	mortality
<i>Histopathological evaluation for autoimmune reactions 5 weeks after neonatal Treg depletion, 2 litters naïve transgenic DEREg</i>			
PBS	3	3	
DTX	2	3	
<i>Flow cytometry: Treg number and frequencies, C57BL/6 from 4 litters</i>			
HI 24 h	16	12	3f
<i>Flow cytometry chemokine receptors, transgenic DEREg from 2 litters</i>			
HI 24 h	6	6	1f, 1m
<i>Flow cytometry integrins, transgenic DEREg from 2 litters</i>			
HI 24h	5	5	
<i>*Immunohistochemistry: Treg localization, transgenic DEREg from 5 litters</i>			
HI 24 h	13	12	1f, 3m
<i>Ex vivo assessment of Treg suppressive activity on myeloid cells, transgenic DEREg from 2 litters</i>			
HI 24 h	4	4	
<i>Depletion efficiency 24h after HI (i.e. 48 h after injection), transgenic DEREg from 7 litters</i>			
PBS	9	10	1m
DTX	8	9	2f, 1m
<i>Behavioral outcome: Treg depletion, analysis 3 days and 5 weeks after HI, transgenic DEREg from 12 litters</i>			
Sham	11	9	
PBS	13	13	1m
DTX	12	11	2f, 2m
<i>Immunohistochemistry: Treg depletion, analysis 7 d after HI, transgenic DEREg from 8 litters</i>			
PBS	13	10	1f, 1m
DTX	13	11	1f
<i>#Immunohistochemistry: Treg depletion, analysis 7 d after sham operation, transgenic DEREg from 6 litters</i>			
PBS	8	8	
DTX	8	8	
<i>Immunohistochemistry: DTX injection, analysis 7 d after HI, wildtype DEREg littermates from 10 litters</i>			
PBS	10	11	1f
DTX	11	10	1f
<i>Western Blot: Treg depletion, analysis 7 d after HI, 6 litters DEREg</i>			
PBS	9	8	1m
DTX	10	8	1f, 1m
<i>Immunohistochemistry: Treg depletion, analysis 48 h after HI, 7 litters DEREg</i>			
PBS	11	11	2f, 2m
DTX	11	11	1f, 2m
<i>§Western Blot#: Treg depletion, analysis 48 h after HI, 5 litters DEREg</i>			
PBS	7	8	1m
DTX	7	8	1m

<sup>\*</sup> part of these animals were also used for Treg-sort from spleens for analysis of suppressive activity on effector T cell proliferation and microarray analysis

<sup>#</sup> these animals were also used for evaluation of Treg recovery 6 days after the last DTX injection

<sup>§</sup> these animals were also used for estradiol measurements in serum samples

**Supplemental Table II: Antibodies and dyes used for flow cytometry**

antigen	conjugate	dilution	host / isotype	clone	supplier
<b>Panel 1: Treg number and frequency, C57BL/6</b>					
CD45	Alexa Fluor700	1:200	Rat / IgG2b, kappa	30-F11	BD Biosciences
CD3	Fitc	1:100	Rat / IgG2b, kappa	17A2	eBioscience
CD8a	PerCP	1:100	Rat / IgG2a, kappa	53-6.7	BD Biosciences
CD4	Pacific Blue	1:800	Rat / IgG2a, kappa	RM4-5	BD Biosciences
FvD	APC-C7	1:3000	-	-	eBioscience

Foxp3	PE	1:100	Rat / IgG2a, kappa	FJK-16s	eBioscience
<b>Panel 2: Depletion efficiency, DERE</b>					
CD45	Pacific Blue	1:200	Rat/IgG2b, kappa	30-F11	Biolegend
CD3	PerCP	1:100	Rat / IgG2a, kappa	53-6.7	BD Biosciences
CD4	PE-Cy7	1:400	Rat DA	RM4-5	BD Biosciences
FvD	APC-C7	1:3000	-	-	eBioscience
Foxp3	PE	1:100	Rat / IgG2a, kappa	FJK-16s	eBioscience
<b>Panel 3: Chemokine receptors, DERE</b>					
CD45	Alexa Fluor700	1:200	Rat / IgG2b, kappa	30-F11	BD Biosciences
CD3	PerCP	1:100	Rat / IgG2a, kappa	53-6.7	BD Biosciences
CD4	Pacific Blue	1:800	Rat / IgG2a, kappa	RM4-5	BD Biosciences
CCR4	PE-Cy7	1:200	American Hamster IgG	2G12	Biolegend
CXCR4	APC	1:300	Rat / IgG2b, kappa	L276F12	Biolegend
FvD	APC-C7	1:3000	-	-	eBioscience
<b>Panel 4: Integrins, DERE</b>					
CD45	Alexa Fluor700	1:200	Rat / IgG2b, kappa	30-F11	BD Biosciences
CD3	PerCP	1:100	Rat / IgG2a, kappa	53-6.7	BD Biosciences
CD4	Pacific Blue	1:800	Rat / IgG2a, kappa	RM4-5	BD
CD29	PE	1:600	American Hamster IgG	HMβ1-1	Biolegend
CD49d	APC	1:400	Taz / G2b, kappa	R1-2	BD Biosciences
LFA-1	PE-Cy7	1:600	Rat / IgG1, kappa	H155-78	Biolegend
FvD	APC-C7	1:3000	-	-	eBioscience
<b>Panel 5: Treg sort &amp; suppression of effector T cell proliferation, DERE</b>					
CD4 (s & p)	Pacific Blue	1:800	Rat / IgG2a, kappa	RM4-5	BD Biosciences
Foxp3 (s & p)	GFP	1:100	Rat / IgG2a, kappa	53-6.7	BD Biosciences
CD45.1 (p)	PE	1:400	Mouse/IgG2a, kappa	A20	eBioscience
Cell prolif. dye	eFluor 670	8 ng/μl	-	-	eBioscience
FvD	APC-C7	1:3000	-	-	eBioscience
<b>Panel 6: Treg / CD11b sort &amp; suppression of myeloid cell activation, DERE</b>					
CD4 (s)	PE-Cy7	1:400	Rat DA	RM4-5	BD Biosciences
CD11b (s & r)	eFluor 450	1:100	Rat / IgG2a, kappa	M1/70	eBioscience
Ly6G (r)	APC	1:100	Rat / IgG2a, kappa	1A8	eBioscience
Dihydrorhodamine (r) -	-	2.5 μg/ml	-	-	Sigma
FvD	APC-C7	1:3000	-	-	eBioscience

*s= antibodies used for sort*

*p=antibodies/dyes used for assessment of proliferation*

*r=used for assessment of ROS production in myeloid subtypes*

### Supplemental Table III: Antibodies used for immunohistochemistry

antigen	dilution	reactivity	host	supplier
NeuN	1:100	mouse	rat	Millipore
Olig2	1:100	mouse	rabbit	Millipore
Iba-1	1:1000	mouse/rat	rabbit	Wako
GFAP	1:500	mouse	rat	Invitrogen
CD45	1:100	mouse	rat	BD Biosciences
Laminin	1:250	mouse	rabbit	Novus
CD31	1:200	mouse	rat	BD Biosciences
CD41	1:200	mouse	rat	BioRad
vWF	1:50	mouse	sheep	Abcam

### Supplemental Table IV: Summary of statistical analyses (provided as separate excel sheet)

**Supplemental Table V: Gene set enrichment analysis for female Tregs compared to male Tregs 24 h after HI**

Gene set	Size	NES	FDR
HALLMARK_MYC_TARGETS_V1	196	3,085246	0,000000
HALLMARK_MTORC1_SIGNALING	197	2,380875	0,000000
HALLMARK_OXIDATIVE_PHOSPHORYLATION	181	2,331847	0,000000
HALLMARK_PROTEIN_SECRETION	94	2,327902	0,000000
HALLMARK_G2M_CHECKPOINT	188	2,214622	0,000000
HALLMARK_MYC_TARGETS_V2	58	2,153836	0,000000
HALLMARK_UNFOLDED_PROTEIN_RESPONSE	107	2,143914	0,000000
HALLMARK_PI3K_AKT_MTOR_SIGNALING	104	1,871425	0,001179
HALLMARK_MITOTIC_SPINDLE	194	0,182482	0,001972
HALLMARK_INTERFERON_ALPHA_RESPONSE	89	0,180871	0,001775
HALLMARK_E2F_TARGETS	197	1,730720	0,003539
HALLMARK_DNA_REPAIR	147	0,015595	0,016918
HALLMARK_ANDROGEN_RESPONSE	94	1,558165	0,015864
HALLMARK_INTERFERON_GAMMA_RESPONSE	186	0,152766	0,019248
HALLMARK_ADIPOGENESIS	194	1,471514	0,029146
HALLMARK_IL2_STAT5_SIGNALING	194	1,436459	0,036290
HALLMARK_PEROXISOME	102	1,424741	0,037210
HALLMARK_TNFA_SIGNALING_VIA_NFKB	192	1,396658	0,043397
HALLMARK_ALLOGRAFT_REJECTION	189	1,392955	0,042831
HALLMARK_FATTY_ACID_METABOLISM	152	1,345283	0,060733
HALLMARK_REACTIVE_OXYGEN_SPECIES_PATHWAY	46	0,125543	0,114623
HALLMARK_TGF_BETA_SIGNALING	54	1,145850	0,244749
HALLMARK_UV_RESPONSE_UP	150	1,138779	0,246603
HALLMARK_P53_PATHWAY	194	1,096604	0,310358
HALLMARK_APOPTOSIS	157	1,076840	0,334622
HALLMARK_CHOLESTEROL_HOMEOSTASIS	72	1,038052	0,405191
HALLMARK_UV_RESPONSE_DN	137	0,974498	0,550427
HALLMARK_IL6_JAK_STAT3_SIGNALING	82	0,933775	0,639262
HALLMARK_HEME_METABOLISM	187	0,798783	0,895849

Results for all gene sets in the hallmark gene set collection of the Molecular Signature Database (MSigDB)<sup>5</sup> are shown.

**Supplemental Table VI: Entire data set of gene expression data from microarray analysis.**

**(provided as separate excel sheet)**

## **References**

1. Herz J, Koster C, Crasmoller M, Abberger H, Hansen W, Felderhoff-Muser U, et al. Peripheral t cell depletion by fty720 exacerbates hypoxic-ischemic brain injury in neonatal mice. *Front Immunol.* 2018;9:1696
2. Herz J, Koster C, Reinboth BS, Dzierko M, Hansen W, Sabir H, et al. Interaction between hypothermia and delayed mesenchymal stem cell therapy in neonatal hypoxic-ischemic brain injury. *Brain Behav Immun.* 2018;70:118-130
3. Mulling K, Fischer AJ, Siakaeva E, Richter M, Bordbari S, Spyra I, et al. Neutrophil dynamics, plasticity and function in acute neurodegeneration following neonatal hypoxia-ischemia. *Brain Behav Immun.* 2021;92:234-244
4. Feather-Schussler DN, Ferguson TS. A battery of motor tests in a neonatal mouse model of cerebral palsy. *J Vis Exp.* 2016
5. Liberzon A, Birger C, Thorvaldsdottir H, Ghandi M, Mesirov JP, Tamayo P. The molecular signatures database (msigdb) hallmark gene set collection. *Cell Syst.* 2015;1:417-425